



Relationship between foramen magnum position and locomotion in extant and extinct hominoids



Dimitri Neaux^{a,*}, Thibaut Bienvenu^{b,c}, Franck Guy^b, Guillaume Daver^b, Gabriele Sansalone^{a,d,e}, Justin A. Ledogar^a, Todd C. Rae^f, Stephen Wroe^a, Michel Brunet^{b,c}

^a Function, Evolution and Anatomy Research Lab, School of Environmental and Rural Science, University of New England, Bldg CO2, Armidale, NSW 2351, Australia

^b Institut de Paléoprimatologie, Paléontologie Humaine: Evolution et Paléoenvironnements – UMR CNRS 7262, Université de Poitiers, Poitiers, Bât B35, 6 Rue Michel Brunet, 86073, France

^c Collège de France, Chaire de Paléontologie Humaine, 3 Rue D'Ulm, 75231 Paris, France

^d Department of Sciences, Roma Tre University, Largo San Leonardo Murialdo 1, I-00146 Rome, Italy

^e Center for Evolutionary Ecology, Largo San Leonardo Murialdo 1, I-00146 Rome, Italy

^f Centre for Research in Evolutionary, Social and Inter-Disciplinary Anthropology, University of Roehampton, Holybourne Avenue, London, SW15 4JD, United Kingdom

ARTICLE INFO

Article history:

Received 3 February 2017

Accepted 20 July 2017

Keywords:

Basicranium

Bipedalism

Hominin

Masticatory apparatus

ABSTRACT

From the Miocene *Sahelanthropus tchadensis* to Pleistocene *Homo sapiens*, hominins are characterized by a derived anterior position of the foramen magnum relative to basicranial structures. It has been previously suggested that the anterior position of the foramen magnum in hominins is related to bipedal locomotor behavior. Yet, the functional relationship between foramen magnum position and bipedal locomotion remains unclear. Recent studies, using ratios based on cranial linear measurements, have found a link between the anterior position of the foramen magnum and bipedalism in several mammalian clades: marsupials, rodents, and primates. In the present study, we compute these ratios in a sample including a more comprehensive dataset of extant hominoids and fossil hominins. First, we verify if the values of ratios can distinguish extant humans from apes. Then, we test whether extinct hominins can be distinguished from non-bipedal extant hominoids. Finally, we assess if the studied ratios are effective predictors of bipedal behavior by testing if they mainly relate to variation in foramen magnum position rather than changes in other cranial structures. Our results confirm that the ratios discriminate between extant bipeds and non-bipeds. However, the only ratio clearly discriminating between fossil hominins and other extant apes is that which only includes basicranial structures. We show that a large proportion of the interspecific variation in the other ratios relates to changes in facial, rather than basicranial, structures. In this context, we advocate the use of measurements based only on basicranial structures when assessing the relationship between foramen magnum position and bipedalism in future studies.

© 2017 Elsevier Ltd. All rights reserved.

1. Introduction

1.1. Bipedalism and foramen magnum position

When compared to other hominoids, extant and extinct hominins are characterized by a derived anterior position of the foramen

magnum, highlighting a reorganization of the surrounding basicranial structures (Dart, 1925; Schultz, 1942; Dean and Wood, 1981; Kimbel and Rak, 2010). The discoveries of *Sahelanthropus tchadensis* (Brunet et al., 2002; Guy et al., 2005; Zollikofer et al., 2005) and *Ardipithecus ramidus* (White et al., 1994; Suwa et al., 2009; Kimbel et al., 2014), both of which exhibit an anteriorly placed foramen magnum, show that this conformation was acquired by at least the late Miocene. Previous studies suggested that the anterior position of the foramen magnum in hominins is related to a habitual bipedal

* Corresponding author.

E-mail address: dimitrineaux@gmail.com (D. Neaux).

locomotor behavior (Broca, 1872; Topinard, 1878; Dart, 1925; Broom, 1938; Le Gros Clark, 1955; Tobias, 1967). However, the functional relationship between foramen magnum position and bipedal locomotion remains unclear (Suwa et al., 2009; Ruth et al., 2016). This is because the anterior position of the foramen magnum and obligate bipedalism are only displayed by humans among extant hominoids. Morphofunctional comparative studies of extant primate cranial base structures are thus inherently limited by the unique nature of the foramen magnum position and locomotor behavior of *Homo sapiens* (see Cartmill, 1990).

To address this challenge, Russo and Kirk (2013) tested the hypothesis that an anteriorly positioned foramen magnum is related to bipedalism through a comparison of basicranial anatomy between bipeds and quadrupeds belonging to three mammalian clades: marsupials (e.g., bipedal kangaroos and wallabies vs. quadrupedal marsupials), rodents (e.g., bipedal kangaroo rats and jerboas vs. quadrupedal rodents), and primates (humans vs. other hominoids). They used three ratios to describe the position of the foramen magnum relative to several splanchnocranial structures (i.e., anterior margin of the temporal fossa, posterior aspect of the last molar crown, and midline posterior aspect of hard palate). The results of Russo and Kirk (2013) demonstrated that, when compared to their quadrupedal relatives, bipedal marsupials, rodents, and primates have a foramen magnum that is more anteriorly positioned (see also Brunet et al., 2002; Suwa et al., 2009; Kimbel and Rak, 2010).

Ruth et al. (2016) challenged the findings of Russo and Kirk (2013), arguing that the chosen ratios did not accurately relate to foramen magnum position, but instead correspond to changes in other cranial structures. Ruth et al. (2016) notably asserted that these ratios are more influenced by masticatory apparatus position and size rather than foramen magnum position. Recently, Russo and Kirk (2017) responded to these criticisms by quantifying the position of the foramen magnum using a new metric based on the position of the sphenoccipital synchondrosis. This new ratio has the advantage of being based on basicranial structures only and does not take into account features related to the masticatory apparatus. Using this metric, Russo and Kirk (2017) confirmed their previous results (Russo and Kirk, 2013), stating that a relationship exists between foramen magnum position and bipedalism in mammals.

1.2. Objectives of this study

Objective #1 In this context, our first objective is to assess if the use of a more comprehensive sample of extant hominoid specimens, including extant species for which the ratios have not been measured yet (e.g., *Pan paniscus*, *Gorilla beringei*, *Pongo abelii*, *Symphalangus syndactylus*), allows corroborating Russo and Kirk (2013, 2017) findings. We use linear measurements and the same ratios in order to facilitate comparison of our results with those of previous analyses. We first test the hypothesis (hypothesis 1) that ratios can distinguish humans from non-bipedal extant hominoids. We compute and compare the ratios for *H. sapiens* and 18 other species belonging to *Pan*, *Gorilla*, *Pongo*, *Hylobates*, *Nomascus*, *Symphalangus*, and *Hoolock*. If hypothesis 1 is rejected, the findings of Russo and Kirk (2013, 2017) will not be corroborated when a larger taxonomic group is included in the study. If the results are consistent with hypothesis 1, our study will confirm that the ratios proposed by Russo and Kirk (2013, 2017) distinguish bipedal (*H. sapiens*) from non-bipedal extant hominoids.

Objective #2 Russo and Kirk (2013, 2017) also suggested that their ratios may be good proxies with which to appraise bipedalism in fossil hominins (Ross and Henneberg, 1995; Nevell and Wood,

2008; Kimbel and Rak, 2010). We compute the ratios proposed by Russo and Kirk (2013, 2017) in a sample of extinct hominins possessing a wide variety of basicranial shapes in order to appraise this statement. We test the hypothesis (hypothesis 2) that the values of the ratios can distinguish between extinct hominins and non-bipedal extant hominoids. A rejected hypothesis 2 will indicate that factors, other than locomotor behavior, are likely to play a part in the ratio values. If the results are in line with hypothesis 2, our study will confirm that the studied ratios are good descriptors of bipedalism in extinct hominins.

Objective #3 As the ratios defined by Russo and Kirk (2013) have been criticized by Ruth et al. (2016), who asserted that they are likely to be affected by the masticatory apparatus, we test the hypothesis (hypothesis 3) that the ratios mainly describe variation in foramen magnum position rather than changes in facial structures. We quantify the variation in the structures related to the studied ratios using geometric morphometric methods on 3D homologous landmarks. If a significant proportion of the variation is related to landmarks located on the face, hypothesis 3 will be rejected and the masticatory apparatus is likely to influence the ratios that include facial features. If most of the variation is related to basicranial landmarks, notably basion, results will be in line with hypothesis 3.

2. Material and methods

2.1. Studied sample

The sample consists of 171 crania, including 157 extant hominoid specimens belonging to 19 different species (Table 1). The remaining crania belong to extinct taxa. All extant individuals were determined to be adults based on the full eruption of the third molars. These specimens are housed in the American Museum of Natural History (New York, USA), the National Museum of Natural

Table 1
Number of specimens for each species included in the studied sample, including catalog numbers for fossil specimens.

Species	Number	Fossil specimens
<i>Homo sapiens</i>	24	
<i>Pan troglodytes</i>	26	
<i>Pan paniscus</i>	13	
<i>Gorilla gorilla</i>	23	
<i>Gorilla beringei</i>	11	
<i>Pongo pygmaeus</i>	19	
<i>Pongo abelii</i>	5	
<i>Hylobates lar</i>	3	
<i>Hylobates muelleri</i>	3	
<i>Hylobates agilis</i>	3	
<i>Hylobates klossii</i>	3	
<i>Hylobates alibarbis</i>	2	
<i>Hylobates moloch</i>	3	
<i>Hylobates pileatus</i>	2	
<i>Nomascus leucogenys</i>	3	
<i>Nomascus concolor</i>	4	
<i>Nomascus gabriellae</i>	1	
<i>Symphalangus syndactylus</i>	7	
<i>Hoolock hoolock</i>	2	
<i>Sahelanthropus tchadensis</i>	1	TM 266-01-060-1
<i>Australopithecus africanus</i>	1	STS 5
<i>Paranthropus aethiopicus</i>	1	KNM-WT 17000
<i>Paranthropus boisei</i>	2	KNM-ER 406, OH 5
<i>Homo habilis</i>	1	KNM-ER 1813
<i>Homo erectus</i>	3	KNM-ER 3733, KNWT-15000, D2700
<i>Homo heidelbergensis</i>	2	Kabwe 1, Petralona 1
<i>Homo neanderthalensis</i>	2	La Ferrassie 1, La-Chapelle-aux-Saints 1
Early <i>Homo sapiens</i>	1	Skhul V

History (Washington, USA), the Natural History Museum (London, UK), the Institut de Paléoprimateologie, Paléontologie Humaine: Evolution et Paléoenvironnements (Poitiers, France), and the Musée Royal de l'Afrique Centrale (Tervuren, Belgium). The list of specimens, including museum specimen number, sex, and location, can be found in the [Supplementary Online Material \(SOM\) Table S1](#). In order to assess shape variations in *H. sapiens*, we used a sample including specimens belonging to different populations ([SOM Table S1](#)). The human sample comprises six morphologically 'extreme' specimens, i.e., individuals exhibiting the largest distances from the consensus shape and the largest pairwise distances from each other, in a principal component analysis of 88 geographically diverse *H. sapiens* crania by [Ledogar et al. \(2016\)](#). The inclusion of these 'extreme' specimens allowed taking into account the variation of cranial shape in humans. The sample also includes 14 extinct hominins belonging to nine different species ([Table 1](#)). For most of the specimens, we worked with three-dimensional (3D) virtual representations in PLY file format generated from computed tomography (CT) scans, with pixel size and slice thickness adjusted according to the cranial size of each specimen ranging from 0.3 mm to 1 mm. Data were taken on virtual reconstructions for three extinct hominins (TM 266-01-060-1, STS 5, and OH 5). Details of these reconstructions can be found in [Zollikofer et al. \(2005\)](#) for TM 266-01-060-1 and in [Wroe et al. \(2010\)](#) for STS 5 and OH 5. Finally, for three other extinct hominin specimens (KNM-ER 1813, D2700, and La-Chapelle-aux-Saints 1), we worked with research quality casts.

2.2. Data acquisition

The 3D virtual representations were placed in norma basilaris using the Avizo v6.0 software. First, the Frankfort Horizontal plane (FHP) was defined between the right and left porion (most lateral point at the center of the upper margin of the external auditory meatus) and the left orbitale (lowest point on the orbital margin) using the 'fit to points' option of the 'oblique slice' tool. If the porion was missing on one side, as is the case in a few fossil specimens, its counterpart on the contralateral side of the cranium was mirrored relative to the midsagittal plane. Snapshots were taken perpendicular to the FHP (i.e., in norma basilaris) with the 'perspective' tool sets on 'orthogonal view' in order to avoid any distortion related to perspective. The research quality casts of KNM-ER 1813, D2700, and La-Chapelle-aux-Saints 1 were photographed following the protocol set by [Russo and Kirk \(2013\)](#), which also considers the plane perpendicular to the FHP to define the norma basilaris. As several specimens (STS 5, KNM-WT 17000, and OH 5) were available both as 3D virtual representations and as casts, we were able to assess the similarity of the two approaches using a correlation coefficient on landmark coordinates (see below).

Linear measurements on the images were carried out using the NIH ImageJ software ([Schneider et al., 2012](#)). [Russo and Kirk \(2013, 2017\)](#) used four ratios based on the position of the foramen magnum relative to: (1) anterior margin of the temporal fossa, (2) posterior aspect of the last molar crown, (3) midline posterior aspect of hard palate, and (4) midline sphenoparietal synchondrosis. The palate ratio was not included in the present study, as most of the fossil specimens were missing the posterior aspect of the hard palate. To assess cranial size, [Russo and Kirk \(2013\)](#) used the geometric mean of cranial length (L), defined as the prosthionopisthocranion segment, and cranial width (W), defined as bizygomatic width. As the zygomatic arches are broken in many fossil specimens, W was defined here as biporion breadth. We used a correlation coefficient to assess the similarity between bizygomatic width and biporion breadth in 30 extant individuals, i.e., three specimens of each of the following species: *H. sapiens*, *Pan*

troglodytes, *P. paniscus*, *Gorilla gorilla*, *Gorilla beringei*, *Pongo pygmaeus*, *P. abelii*, *Hylobates lar*, *Nomascus concolor*, and *S. syndactylus*. In the present study, the temporal fossa ratio was computed as the mean of the left and right anterior temporal fossa to basion segments (TF1 and TF2) over the geometric mean of L and W ([Fig. 1, Table 2](#)). The molar ratio was computed as the mean of the left and right posterior molar to basion segments (M1 and M2) over the geometric mean of L and W. The basioccipital ratio was computed as the sphenobasion to basion segment (SB) over the geometric mean of L and W. The L, W, TF1, TF2, M1, M2, and SB lengths were all directly obtained from the screen captures of the scans or the digital photographs of the casts. For a few fossil taxa, measurements were only available on one side of the cranium. In this case, only one TF (or one M) was taken into account to compute the ratio. Also, when porion was missing on one side, W was computed as twice the distance between the preserved porion and the midsagittal plane. Finally, the sphenoparietal synchondrosis was not visible in all specimens, so the basioccipital ratio was not computed for the specimens where the sphenobasion could not be confidently identified. These specimens are identified in [SOM Table S1](#).

Cranial base shape was also described using eight two-dimensional landmark coordinates ([Fig. 1, Table 2](#)). Landmarks were placed on the images with tpsDig v2.32 ([Rohlf, 2015](#)). If a landmark were missing, its counterpart on the other side of the cranium was mirrored relative to the midsagittal plane. To validate this approach, we estimated a landmark on five complete specimens belonging to five different species (i.e., *H. sapiens*, *P. troglodytes*, *G. gorilla*, *Pon. pygmaeus*, *H. lar*). We tested for differences between the estimated landmarks and the real ones using a MANOVA. To test for measurement and landmark repeatability, one female *G. gorilla* specimen was resampled three times on three different days.

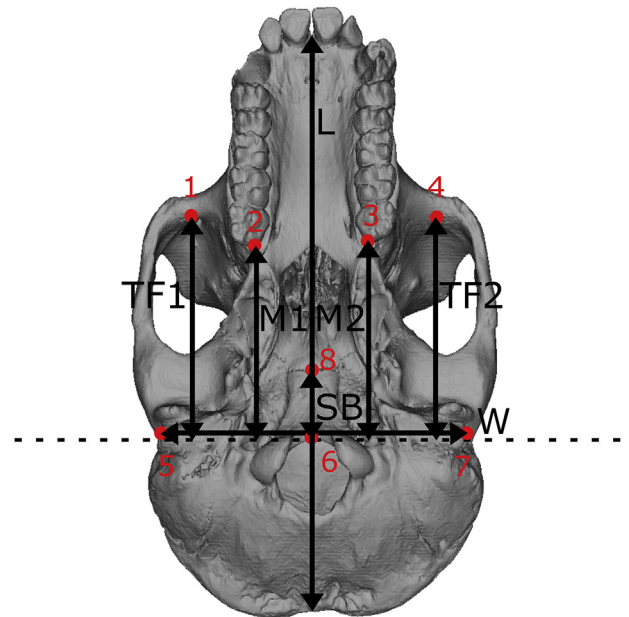


Figure 1. *Gorilla* cranium in norma basilaris showing the landmarks and the measurements taken on each specimen. 1 = Anterior temporal fossa right, 2 = posterior molar right, 3 = posterior molar left, 4 = anterior temporal fossa left, 5 = porion right, 6 = basion, 7 = porion left, 8 = sphenobasion, dashed line = basion line, L = cranial length, W = cranial width, TF1 and TF2 = anterior temporal fossa to basion segments, M1 and M2 = posterior molar to basion segments, SB = sphenobasion to basion segment.

Table 2
Definition of landmarks.

Landmark	Number	Definition
Anterior temporal fossa	1, 4	Most anterior point of the temporal fossa
Posterior molar	2, 3	Most posterior point of the last molar
Porion	5, 7	Most lateral point at the center of the upper margin of the external auditory meatus
Basion	6	Most anterior midsagittal point of the foramen magnum
Sphenobasion	8	Midline point of the spheno-occipital synchondrosis

2.3. Analyses

Species belonging to the genus *Hylobates* have been previously described as morphologically uniform (Groves, 1972; Chatterjee, 2009; Fleagle, 2013; Neaux, 2017). We tested for differences in the ratios between the seven studied species of *Hylobates* using ANOVAs to define if they should be computed separately or together in the following analyses. We did the same with the three species of the genus *Nomascus*, also belonging to the Hylobatidae family.

Contrary to Russo and Kirk (2013, 2017), we compared more than two groups for each ratio. The significance of the ratios differences was therefore evaluated using a pairwise permuted ANOVA applying the wrapper function `pwperanovac()` (Sansalone et al., 2016), available in SOM S1. Holm correction was performed, to account for unbalanced sample size (Holm, 1979). As only two specimens of *Hoolock* were available, this genus was not included in the pairwise ANOVAs. Ratio differences between groups have been depicted through boxplots using the wrapper function `boxord()` (Sansalone et al., 2016), available in SOM S1. Statistics were performed in the R statistical environment (R Development Core Team, 2016).

The analysis of landmark variations was performed using MorphoJ v1.06 (Klingenberg, 2011). Symmetric configurations from original landmark coordinates and a Procrustes superimposition, including the specimens for which the temporal fossa, molar, and basioccipital ratios have been measured, were computed. Principal component analysis (PCA) was performed to visualize the overall morphological variations and the distribution of individuals in the shape space. We computed the influence of any single landmark on

each significant principal component (PC) as the square root of the sum of the squared coordinate loadings for that landmark (Baab and McNulty, 2009; Bienvenu et al., 2011).

3. Results

3.1. Error tests

Results show a significant relationship between the results of CT and photographic methods (STS 5: $r = 0.95$, $p < 0.01$; KNM-WT 17000: $r = 0.98$, $p < 0.01$; OH 5: $r = 0.98$, $p < 0.01$). Therefore, photographs of the casts of KNM-ER 1813, D2700, and La-Chapelle-aux-Saints 1 were included in the study. The relationship between biporion breadth and bizygomatic width is also significant ($r = 0.97$, $p < 0.01$), showing that the first distance is a good proxy for the second. MANOVA results show no significant differences between mirror-estimated and actual landmarks (Wilk's $\lambda = 0.87$, $F[2,7] = 0.48$, $p = 0.63$), allowing estimates to be used for those specimens missing one side. Measurement errors show no significant differences between the repeated samples for linear measurements ($F[2,15] = 0.01$, $p = 0.99$) or landmarks (Wilk's $\lambda = 0.99$, $F[4,34] = 0.01$, $p = 0.99$).

No significant difference was found between the seven species of *Hylobates*, nor between the three species of *Nomascus* for the temporal fossa (respectively, $F[6,11] = 0.67$, $p = 0.72$ and $F[4,2] = 2.23$, $p = 0.23$), molar ($F[6,11] = 1.59$, $p = 0.22$ and $F[4,2] = 0.91$, $p = 0.46$), and basioccipital ratios ($F[6,11] = 2.42$, $p = 0.12$ and $F[4,2] = 0.91$, $p = 0.46$). For this reason, the species belonging to *Hylobates* were computed together in the following analyses, as were the species belonging to *Nomascus*.

3.2. Objective #1

Temporal fossa (Fig. 2), molar (Fig. 3), and basioccipital ratios (Fig. 4) distinguish humans from non-bipedal extant hominoids (Table 3). There are significant pairwise differences between *H. sapiens* and all the other extant taxa (Table 4). Significant differences exist also between non-bipedal extant species.

3.3. Objective #2

The temporal fossa ratio (Fig. 2) distinguishes bipeds (extant and extinct) from non-bipedal taxa, with two exceptions:

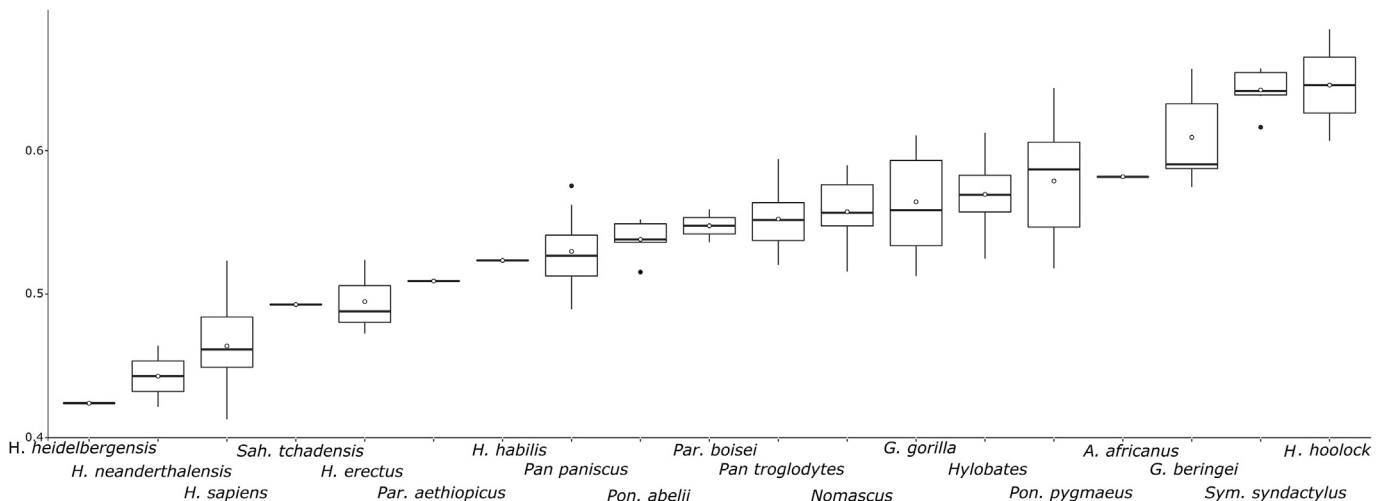


Figure 2. Boxplot of the temporal fossa (TF) ratio in the studied sample. Bottom and top of the boxes are the first and third quartiles, the horizontal black lines represent the median, the whiskers represent the minimum and maximum values, white dots are the mean, and black dots are the outliers.

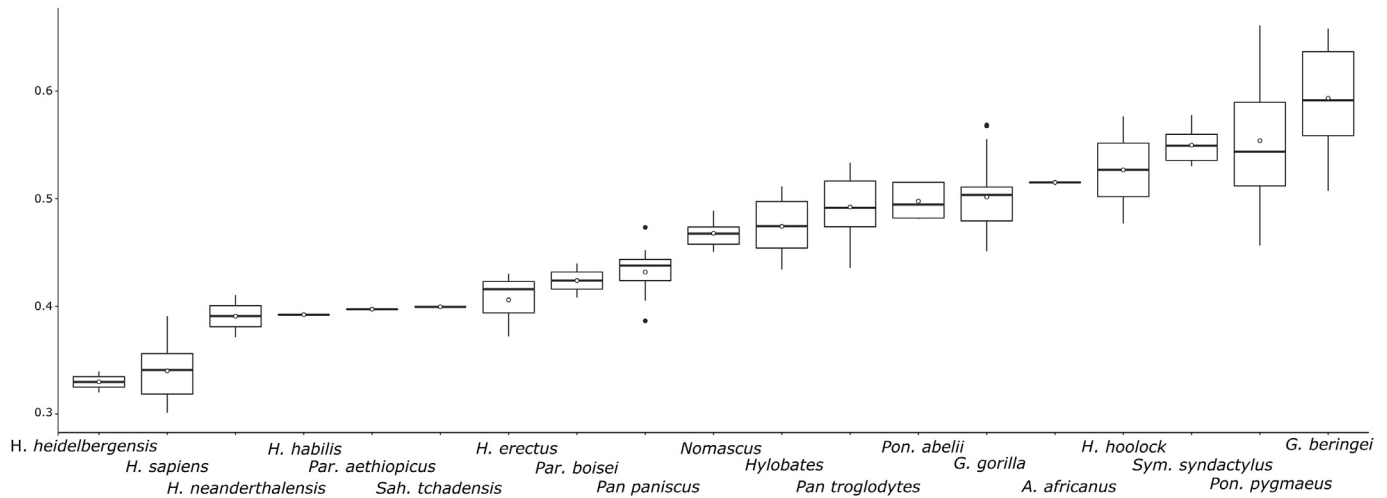


Figure 3. Boxplot of molar (M) ratio in the studied sample. Bottom and top of the boxes are the first and third quartiles, the horizontal black lines represent the median, the whiskers represent the minimum and maximum values, white dots are the mean, and black dots are the outliers.

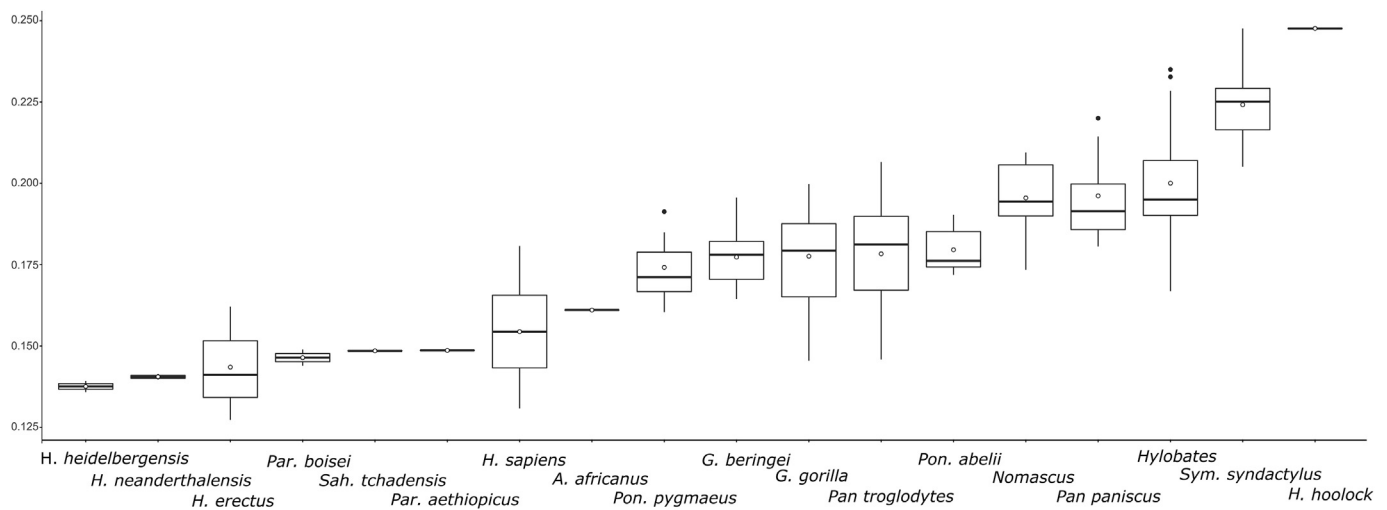


Figure 4. Boxplot of basioccipital (BO) ratio in the studied sample. Bottom and top of the boxes are the first and third quartiles, the horizontal black lines represent the median, the whiskers represent the minimum and maximum values, white dots are the mean, and black dots are the outliers.

Australopithecus africanus and *Paranthropus boisei* fall within the range of extant non-human hominoids (Fig. 2, Table 3). Similarly, *A. africanus* is also found within the non-hominin extant hominoid range for the molar ratio (Fig. 3, Table 3). Having relatively low values when compared to other non-bipedal taxa, a considerable number of *P. paniscus* specimens fall within the range of extinct hominins for the temporal fossa (Fig. 2) and molar (Fig. 3) ratios. The basioccipital ratio (Fig. 4) more clearly distinguishes bipeds (extant and extinct) from non-bipedal taxa, with only few specimens of *G. gorilla* and *P. troglodytes* falling into the hominin range. The value for *A. africanus* stays higher than those of other fossil specimens but, contrary to what is observed for the temporal fossa and molar ratios, it stays well under the means of extant non-bipedal taxa.

3.4. Objective #3

In the PCA, PC1 and PC2 explain, respectively, 65.89% and 14.23% of the total variance (Fig. 5). On PC1, toward positive scores, the anterior temporal fossa is displaced laterally and the posterior

molar landmark is displaced laterally and posteriorly. Porion is displaced laterally and anteriorly, and basion and sphenobasion are displaced anteriorly. On PC2, toward higher scores, the anterior temporal fossa is displaced anteriorly and the posterior molar is displaced medially and posteriorly. Porion is displaced anteriorly, and basion and sphenobasion are displaced posteriorly. The weightings of landmarks on PC1 and PC2 are presented in Table 5. A substantial proportion of the changes on PC1 are associated with the posterior molar landmarks (2, 3). On PC2, changes are also mostly related to basion (6) and the anterior cranial fossa landmarks (1, 4).

4. Discussion

4.1. Foramen magnum position and locomotion

Our findings support hypothesis 1, as we found significant differences for the temporal fossa, molar, and basioccipital ratios between bipedal (*H. sapiens*) and non-bipedal extant hominoids. The present study was therefore able to replicate the findings of Russo

Table 3

Mean, 95% confidence interval for the mean (95% CI), standard deviation (SD), minimum value (Min) and maximum value (Max) for the temporal fossa (TF), molar (M), and basioccipital (BO) ratios in each studied taxa.

TF ratio	Mean	95% CI	SD	Min	Max
<i>Homo sapiens</i>	0.46	0.01	0.03	0.41	0.52
<i>Pan troglodytes</i>	0.55	0.01	0.02	0.52	0.59
<i>Pan paniscus</i>	0.53	0.01	0.03	0.49	0.57
<i>Gorilla gorilla</i>	0.56	0.01	0.03	0.51	0.61
<i>Gorilla beringei</i>	0.61	0.02	0.03	0.57	0.66
<i>Pongo pygmaeus</i>	0.58	0.02	0.04	0.52	0.64
<i>Pongo abelii</i>	0.54	0.01	0.01	0.52	0.55
<i>Hylobates</i> spp.	0.57	0.01	0.02	0.52	0.61
<i>Nomascus</i> spp.	0.56	0.02	0.02	0.52	0.59
<i>Symphalangus syndactylus</i>	0.64	0.01	0.02	0.61	0.66
<i>Hoolock hoolock</i>	0.65	0.08	0.05	0.61	0.68
<i>Sahelanthropus tchadensis</i>	0.49	–	–	–	–
<i>Australopithecus africanus</i>	0.58	–	–	–	–
<i>Paranthropus aethiopicus</i>	0.51	–	–	–	–
<i>Paranthropus boisei</i>	0.55	0.02	0.02	0.54	0.56
<i>Homo habilis</i>	0.52	–	–	–	–
<i>Homo erectus</i>	0.49	0.03	0.03	0.47	0.52
<i>Homo heidelbergensis</i>	0.42	0.00	0.00	0.42	0.42
<i>Homo neanderthalensis</i>	0.44	0.04	0.03	0.42	0.46
M ratio	Mean	95% CI	SD	Min	Max
<i>Homo sapiens</i>	0.34	0.01	0.02	0.30	0.39
<i>Pan troglodytes</i>	0.49	0.01	0.03	0.44	0.53
<i>Pan paniscus</i>	0.43	0.01	0.02	0.38	0.47
<i>Gorilla gorilla</i>	0.50	0.01	0.03	0.45	0.57
<i>Gorilla beringei</i>	0.59	0.03	0.05	0.51	0.66
<i>Pongo pygmaeus</i>	0.55	0.02	0.05	0.46	0.66
<i>Pongo abelii</i>	0.50	0.01	0.02	0.48	0.52
<i>Hylobates</i> spp.	0.47	0.01	0.03	0.43	0.51
<i>Nomascus</i> spp.	0.47	0.01	0.01	0.45	0.49
<i>Symphalangus syndactylus</i>	0.55	0.01	0.02	0.53	0.58
<i>Hoolock hoolock</i>	0.53	0.10	0.07	0.48	0.58
<i>Sahelanthropus tchadensis</i>	0.40	–	–	–	–
<i>Australopithecus africanus</i>	0.52	–	–	–	–
<i>Paranthropus aethiopicus</i>	0.40	–	–	–	–
<i>Paranthropus boisei</i>	0.42	0.03	0.02	0.41	0.44
<i>Homo habilis</i>	0.39	–	–	–	–
<i>Homo erectus</i>	0.41	0.03	0.03	0.37	0.43
<i>Homo heidelbergensis</i>	0.33	0.02	0.01	0.32	0.34
<i>Homo neanderthalensis</i>	0.39	0.04	0.03	0.37	0.41
BO ratio	Mean	95% CI	SD	Min	Max
<i>Homo sapiens</i>	0.15	0.01	0.01	0.13	0.18
<i>Pan troglodytes</i>	0.18	0.01	0.02	0.15	0.21
<i>Pan paniscus</i>	0.20	0.01	0.02	0.18	0.22
<i>Gorilla gorilla</i>	0.18	0.01	0.02	0.15	0.20
<i>Gorilla beringei</i>	0.18	0.01	0.01	0.16	0.20
<i>Pongo pygmaeus</i>	0.17	0.01	0.01	0.16	0.19
<i>Pongo abelii</i>	0.18	0.01	0.01	0.17	0.19
<i>Hylobates</i> spp.	0.20	0.01	0.02	0.17	0.24
<i>Nomascus</i> spp.	0.20	0.01	0.01	0.17	0.21
<i>Symphalangus syndactylus</i>	0.22	0.01	0.01	0.21	0.25
<i>Hoolock hoolock</i>	0.25	–	–	–	–
<i>Sahelanthropus tchadensis</i>	0.15	–	–	–	–
<i>Australopithecus africanus</i>	0.16	–	–	–	–
<i>Paranthropus aethiopicus</i>	0.15	–	–	–	–
<i>Paranthropus boisei</i>	0.15	0.00	0.00	0.14	0.15
<i>Homo habilis</i>	–	–	–	–	–
<i>Homo erectus</i>	0.14	0.02	0.02	0.13	0.16
<i>Homo heidelbergensis</i>	0.14	0.00	0.00	0.14	0.14
<i>Homo neanderthalensis</i>	0.14	0.00	0.00	0.14	0.14

and Kirk (2013, 2017) using a more comprehensive sample. Our work supports the hypothesis that the ratios proposed by Russo and Kirk (2013, 2017) are reliable indicators of bipedalism in extant hominoids. However, our results show that significant differences also exist between non-bipedal extant hominoids, underlining that the studied ratios are influenced by factors other than bipedalism. It is not certain that the variety of locomotor

behavior found in apes, other than bipedalism, can explain these differences. Indeed, previous works found similar foramen magnum positions in *Gorilla* and *Pongo* (Dean and Wood, 1982), two taxa possessing very different locomotor behaviors (Cant, 1987; Remis, 1998; Thorpe and Crompton, 2006). Conversely, allometry can be one of the factors influencing these interspecific differences, as simple ratios do not remove the frequently non-linear (i.e., allometric) correlations between size and shape. Allometry may explain the differences between taxa differing greatly in size, such as hylobatids and great apes (Leslie and Shea, 2016) or *P. paniscus* and the other great apes (Shea, 1983; Lieberman et al., 2007). Another reason, advanced by Ruth et al. (2016) for the temporal fossa and molar ratios, is that other cranial morphological structures, not located in the basicranium, may influence the computed values.

Our results for the basioccipital ratio are in line with hypothesis 2, as this metric differentiates bipeds (extant and extinct) from non-bipedal taxa with only a few specimens of *G. gorilla* and *P. troglodytes* falling within the hominin range. The present study confirms that the basioccipital ratio defined by Russo and Kirk (2017) is an appropriate indicator of bipedalism in extinct hominins. For the temporal and the molar ratios, two extinct hominoids are in the range of non-bipedal extant hominoids: *A. africanus* and *Par. boisei*. This suggests once again that morphological features unrelated to basicranial structures or locomotor behavior are likely to influence the values of these ratios.

Our landmark study does not support hypothesis 3, as it shows that an important part of the variation in the structures related to the studied ratios is related to the face and the masticatory apparatus (anterior temporal fossa and posterior molar landmarks). However, basion, located on the foramen magnum, represents a great part of the variations on PC2. These results may explain the values for the temporal fossa and molar ratios in *A. africanus* and, to a lesser extent, those of *Par. boisei* for the temporal fossa ratio. These two taxa display higher ratio values than expected considering the position of their foramen magnum relative to the cranial base (Dean and Wood, 1981, 1982).

4.2. Problems related to the temporal fossa and molar ratios

Australopithecus africanus exhibits an anteriorly positioned zygomatic root complex, which increases the leverage for the superficial masseter (Rak, 1983; Schwartz and Tattersall, 2005; Smith et al., 2015). In *Par. boisei*, the zygomatic arch is widely flared and anteriorly positioned (Rak, 1983; Schwartz and Tattersall, 2005; Smith et al., 2015; Rak and Marom, 2017). The study of the shape space shows great interspecific variation in the projection of the zygomatic relative to basicranial structures, which are likely to influence the temporal fossa ratio (Fig. 4, Table 5). This explains why *A. africanus* and *Par. boisei*, both possessing anteriorly projected zygomatic arches, display high temporal fossa ratios that fall within the range of non-bipedal hominoids. This result is in line with the findings of Russo and Kirk (2017) comparing the temporal fossa ratio in two rodents belonging to the Anomaluroida clade: the bipedal *Pedetes* and the quadrupedal *Anomalurus* (see Fabre et al., 2012, 2013). Russo and Kirk (2017) found that *Anomalurus* has a significantly lower temporal fossa ratio than *Pedetes*. They proposed that this result, which is contrary to their expectations, is due to the far anterior position of the anterior margin of the temporal fossa in *Pedetes*. This example in anomaluroids, as well as in *A. africanus* and *Par. boisei* in the present work, suggests that the temporal fossa ratio is strongly influenced by changes in the relative position of splanchnocranial (i.e., facial) structures. In this sense, they are in line with the criticisms forwarded by Ruth et al.

Table 4

P-values of the non-parametric pairwise ANOVAs between the extant studied species for the temporal fossa (TF), molar (M), and basioccipital (BO) ratios.^a

	<i>Pan troglodytes</i>	<i>Pan paniscus</i>	<i>Gor. gorilla</i>	<i>Gor. beringei</i>	<i>Pon. pygmaeus</i>	<i>Pon. abelii</i>	<i>Hylobates</i> spp.	<i>Nomascus</i> spp.	<i>Sym. syndactylus</i>
TF ratio									
<i>H. sapiens</i>	<0.01	<0.01	<0.01	<0.01	<0.01	<0.01	<0.01	<0.01	<0.01
<i>Pan troglodytes</i>		0.17	0.13	<0.01	0.10	0.15	0.30	0.57	<0.01
<i>Pan paniscus</i>			0.08	<0.01	<0.01	0.51	<0.01	0.50	<0.01
<i>Gor. gorilla</i>				<0.01	0.18	0.08	0.55	0.56	<0.01
<i>Gor. beringei</i>					0.51	0.03	0.01	0.04	0.37
<i>Pon. pygmaeus</i>						0.53	0.36	0.15	0.01
<i>Pon. abelii</i>							0.24	0.14	0.03
<i>Hylobates</i> spp.								0.23	<0.01
<i>Nomascus</i> spp.									<0.01
M ratio									
<i>H. sapiens</i>	<0.01	<0.01	<0.01	<0.01	<0.01	<0.01	<0.01	<0.01	<0.01
<i>Pan troglodytes</i>		<0.01	0.28	<0.01	<0.01	0.69	0.63	0.50	<0.01
<i>Pan paniscus</i>			<0.01	<0.01	<0.01	<0.01	<0.01	0.05	<0.01
<i>Gor. gorilla</i>				<0.01	<0.01	0.80	0.12	0.15	0.02
<i>Gor. beringei</i>					0.82	0.04	<0.01	<0.01	0.68
<i>Pon. pygmaeus</i>						0.63	<0.01	<0.01	0.84
<i>Pon. abelii</i>							0.85	0.14	0.05
<i>Hylobates</i>								0.50	0.01
<i>Nomascus</i>									0.01
BO ratio									
<i>H. sapiens</i>	<0.01	<0.01	<0.01	<0.01	<0.01	<0.01	<0.01	<0.01	<0.01
<i>Pan troglodytes</i>		0.10	0.84	0.45	0.87	0.02	0.35	<0.01	0.02
<i>Pan paniscus</i>			0.03	0.04	0.93	0.57	0.93	0.08	0.03
<i>Gor. gorilla</i>				0.54	0.80	0.01	0.37	<0.01	0.04
<i>Gor. beringei</i>				0.50	0.63	0.04	0.14	<0.01	0.05
<i>Pon. pygmaeus</i>					0.39	0.01	0.12	<0.01	0.06
<i>Pon. abelii</i>						0.62	0.87	0.04	0.07
<i>Hylobates</i> spp.							0.56	0.16	0.08
<i>Nomascus</i> spp.								0.11	0.09

^a P-values significant at 0.05 are in bold.

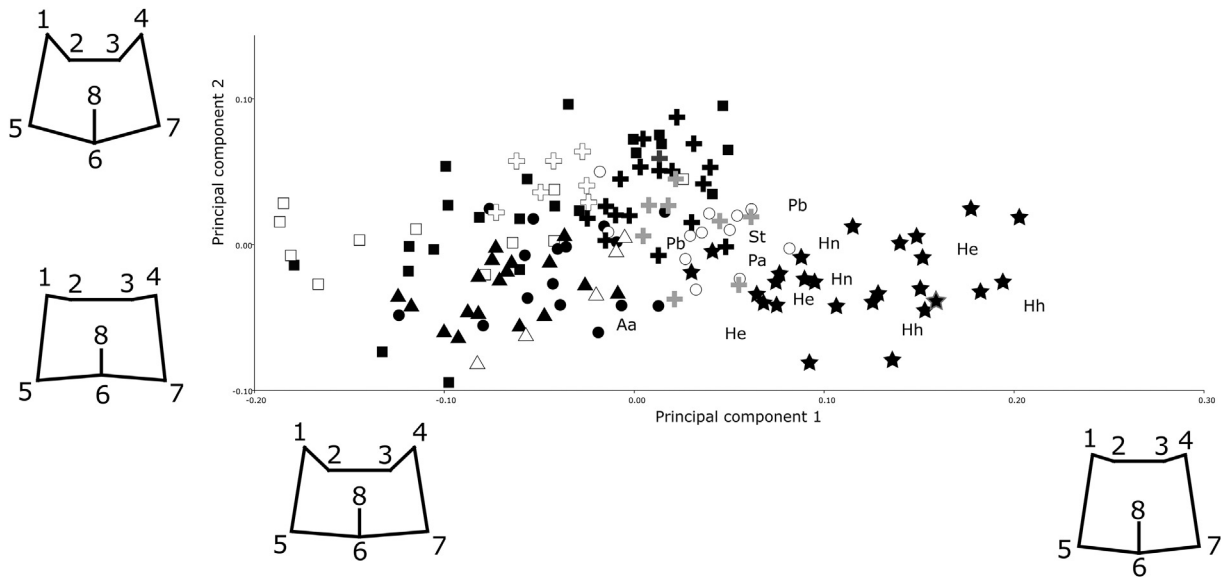


Figure 5. Principal component analysis showing the repartition of the specimens in the PC1–PC2 morphospace. Stars = *Homo sapiens*, black dots = *Pan troglodytes*, white dots = *Pan paniscus*, black squares = *Gorilla gorilla*, white squares = *Gorilla beringei*, black triangles = *Pongo pygmaeus*, white triangles = *Pongo abelii*, black crosses = *Hylobates* spp., light gray crosses = *Nomascus* spp., white crosses = *Symphalangus syndactylus*, dark gray cross = *Hoolock hoolock*, St = *Sahelanthropus tchadensis*, Aa = *Australopithecus africanus*, Pa = *Paranthropus aethiopicus*, Pb = *Paranthropus boisei*, He = *Homo erectus*, Hh = *Homo heidelbergensis*, Hn = *Homo neanderthalensis*. The star with a gray border is Skhul V. The wireframes display the shape changes on each axis. 1 = anterior temporal fossa right, 2 = posterior molar right, 3 = posterior molar left, 4 = anterior temporal fossa left, 5 = porion right, 6 = basion, 7 = porion left, 8 = sphenobasion.

(2016) that Russo and Kirk’s (2013, 2017) temporal fossa ratio is influenced by cranial structures other than the foramen magnum.

STS 5 has been described as being exceptionally prognathic when compared to other specimens of *A. africanus*, such as STS 71 and STS 52a (Rak, 1983; Kimbel and White, 1988; Kimbel et al.,

2004). In STS 5, the anteriorly positioned premaxilla is associated with an anteriorly positioned third molar, as these structures are both related to the anteroposterior position of the hard palate (McCollum et al., 1993; McCollum, 2000; Cobb, 2008). The anterior position of the subnasal part of the face in STS 5 is therefore

Table 5

Loadings of landmarks on each significant principal component. The principal component analysis was performed on the Procrustes coordinates of the landmarks describing cranial base shape.

Landmark ^a	PC1	PC2
1, 4	0.25	0.46
2, 3	0.51	0.31
5, 7	0.34	0.22
6	0.28	0.47
8	0.19	0.26

^a 1 = Anterior temporal fossa right, 2 = posterior molar right, 3 = posterior molar left, 4 = anterior temporal fossa left, 5 = porion right, 6 = basion, 7 = porion left, 8 = sphenobasion.

associated with (1) an anterior position of the third molars relative to the whole cranium and (2) a reduction of the distance between the temporal fossa and the third molar as revealed by the low score of STS 5 along PC1 in the shape space (Fig. 5). Therefore, the strong subnasal prognathism of STS 5 associated with an anterior position of the third molars may explain its high molar ratio value within the range of non-bipedal hominoids. These findings reveal that the molar ratio, like the temporal fossa ratio, is likely to be influenced by splanchnocranial structures not directly related to the position of the foramen magnum (Ruth et al., 2016).

5. Conclusions

The temporal fossa, molar, and basioccipital ratios defined by Russo and Kirk (2013, 2017) are reliable descriptors of bipedalism in extant hominoids (hypothesis 1). The basioccipital ratio is the only reliable ratio when extinct specimens are included (hypothesis 2), as a strong component of the variation within the temporal fossa and molar ratios is likely to be related to the masticatory apparatus (hypothesis 3). This major problem associated with the use of the temporal fossa and molar ratios was already identified by Russo and Kirk (2013:659), who noted that their “measures of relative basion position could arguably reflect variation in craniofacial morphology unrelated to foramen magnum position.” On that point, our study is in line with Ruth et al. (2016), who noted that these ratios mostly describe the relative positioning of splanchnocranial structures. Importantly, these structures are highly influenced by masticatory adaptations. For example, studies of bite force leverage in the crania of *A. africanus* and *Par. boisei* (e.g., Demes and Creel, 1988; Eng et al., 2013; Smith et al., 2015) suggest that both species, and *Paranthropus* in particular, could generate bite forces more efficiently than extant chimpanzees, in part due to their derived zygomatic morphology. Indeed, the zygomatic is shaped by numerous selective forces, including diet and feeding, visual acuity, and facial mobility (Dechow and Wang, 2016; Ledogar et al., 2017; Rak and Marom, 2017; Weber and Krenn, 2017).

The use of metrics based on the facial traits to assess the position of midsagittal basicranial structures is also made less relevant by the fact that several studies have found that the midline cranial base and the face may belong to different modules, possibly influenced by different developmental and functional integration pathways (Bastir and Rosas, 2006; Gkantidis and Halazonetis, 2011; Neaux et al., 2013). In this context, the use of measurements only based on basicranial structures, such as basioccipital ratios (Russo and Kirk, 2017) or the position of basion relative to the bicarotid chords (Schaefer, 1999; Ahern, 2005), are probably more reliable means with which to assess foramen magnum position. An alternative solution may lie in the continued development of 3D geometric morphometric analysis of basicranial structures (Aristide et al., 2015), as well as in the generalization of 3D craniofacial morphological integration studies (Bastir and Rosas, 2016; Neaux, 2017).

Acknowledgments

We thank the Smithsonian's Division of Mammals (K. Helgen) and Human Origins Program (M. Tocheri) for the scans of the National Museum of Natural History specimens used in this research (<http://humanorigins.si.edu/evidence/3d-collection/primates>). These scans were acquired through the support of the Smithsonian 2.0 Fund and the Smithsonian's Collections Care and Preservation Fund. We also wish to thank the following institutions and people for allowing us the access to their specimens: D.E. Lieberman, the Peabody Museum of Archaeology and Ethnology at Harvard, the American Museum of National History, the Natural History Museum, the Institut de Paléoprimatologie, Paléontologie Humaine: Evolution et Paléoenvironnements, E. Gilissen, W. Wendelen, the Musée Royal de l'Afrique Centrale, and the NESPOS society. We finally thank the Editor (D.M. Alba), an Associate Editor, a reviewer (G.A. Russo), and an anonymous reviewer for their valuable comments on an earlier draft of this manuscript. Some of the scans of humans have been obtained through a grant (NSF-BCS-0725126) awarded to D.S. Strait. This work was supported by an Australian Research Council (ARC) Discovery grant (DP140102659) to S.W.

Supplementary Online Material

Supplementary online material related to this article can be found at <http://dx.doi.org/10.1016/j.jhevol.2017.07.009>.

References

Ahern, J.C.M., 2005. Foramen magnum position variation in *Pan troglodytes*, Plio-Pleistocene hominids, and recent *Homo sapiens*: implications for recognizing the earliest hominids. *Am. J. Phys. Anthropol.* 127, 267–276.

Aristide, L., dos Reis, S.F., Machado, A.C., Lima, I., Lopes, R.T., Perez, S.I., 2015. Encephalization and diversification of the cranial base in platyrrhine primates. *J. Hum. Evol.* 81, 29–40.

Baab, K.L., McNulty, K.P., 2009. Size, shape, and asymmetry in fossil hominins: the status of the LB1 cranium based on 3D morphometric analyses. *J. Hum. Evol.* 57, 608–622.

Bastir, M., Rosas, A., 2006. Correlated variation between the lateral basicranium and the face: A geometric morphometric study in different human groups. *Archaeol. Oral Biol.* 51, 814–824.

Bastir, M., Rosas, A., 2016. Cranial base topology and basic trends in the facial evolution of *Homo*. *J. Hum. Evol.* 91, 26–35.

Bienvenu, T., Guy, F., Coudyzer, W., Gilissen, E., Rouldès, G., Vignaud, P., Brunet, M., 2011. Assessing endocranial variations in great apes and humans using 3D data from virtual endocasts. *Am. J. Phys. Anthropol.* 145, 231–246.

Broca, P., 1872. Sur la direction du trou occipital. Description du niveau occipital et du goniomètre occipital. *B. Mem. Soc. Anthropol. Par.* 7, 649–668.

Broom, R., 1938. The Pleistocene anthropoid apes of South Africa. *Nature* 142, 377–379.

Brunet, M., Guy, F., Pilbeam, D., Mackaye, H.T., Likius, A., Ahounta, D., Beauvilain, A., Blondel, C., Bocherens, H., Boisserie, J.-R., de Bonis, L., Coppens, Y., Dejax, J., Denys, C., Durringer, P., Eisenmann, V., Fanone, G., Fronty, P., Geraads, D., Lehmann, T., Lihoreau, F., Louchart, A., Mahamat, A., Merceron, G., Mouchelin, G., Otero, O., Campomanes, P.P., De Leon, M.P., Rage, J.-C., Sapanet, M., Schuster, M., Sudre, J., Tassy, P., Valentin, X., Vignaud, P., Viriot, L., Zazzo, A., Zollikofer, C., 2002. A new hominid from the Upper Miocene of Chad, Central Africa. *Nature* 418, 145–151.

Cant, J.G.H., 1987. Positional behavior of female bornean orangutans (*Pongo pygmaeus*). *Am. J. Primatol.* 12, 71–90.

Cartmill, M., 1990. Human uniqueness and theoretical content in paleoanthropology. *Intl. J. Primatol.* 11, 173–192.

Chatterjee, H.J., 2009. Evolutionary relationships among the gibbons: A biogeographic perspective. In: Whittaker, D., Lappan, S. (Eds.), *The Gibbons. Developments in Primatology: Progress and Prospects*. Springer, New York, pp. 13–36.

Cobb, S.N., 2008. The facial skeleton of the chimpanzee-human last common ancestor. *J. Anat.* 212, 469–485.

Dart, R.A., 1925. *Australopithecus africanus*: the man-ape of southern Africa. *Nature* 115, 195–199.

Dean, M.C., Wood, B.A., 1981. Metrical analysis of the basicranium of extant hominoids and *Australopithecus*. *Am. J. Phys. Anthropol.* 54, 63–71.

Dean, M.C., Wood, B.A., 1982. Basicranial anatomy of Plio-Pleistocene hominids from East and South Africa. *Am. J. Phys. Anthropol.* 59, 157–174.

Dechow, P.C., Wang, Q., 2016. Development, structure, and function of the zygomatic bones: what is new and why do we care? *Anat. Rec.* 299, 1611–1615.

Demes, B., Creel, N., 1988. Bite force, diet, and cranial morphology of fossil hominids. *J. Hum. Evol.* 17, 657–670.

- Eng, C.M., Lieberman, D.E., Zink, K.D., Peters, M.A., 2013. Bite force and occlusal stress production in hominin evolution. *Am. J. Phys. Anthropol.* 151, 544–557.
- Fabre, P.-H., Hautier, L., Dimitrov, D., P Douzery, E.J., 2012. A glimpse on the pattern of rodent diversification: a phylogenetic approach. *BMC Evol. Biol.* 12, 88.
- Fabre, P.-H., Jönsson, K.A., Douzery, E.J.P., 2013. Jumping and gliding rodents: mitogenomic affinities of Pedetidae and Anomaluridae deduced from an RNA-Seq approach. *Gene* 531, 388–397.
- Feagle, J.G., 2013. *Primate Adaptation and Evolution*, 3rd ed. Academic Press, New York.
- Gkantidis, N., Halazonetis, D.J., 2011. Morphological integration between the cranial base and the face in children and adults. *J. Anat.* 218, 426–438.
- Groves, C.P., 1972. Systematics and phylogeny of gibbons. In: Rumbaugh, D. (Ed.), *Gibbon and Siamang*. Karger, Basel, pp. 1–89.
- Guy, F., Lieberman, D.E., Pilbeam, D., Ponce de León, M., Likius, A., Mackaye, H.T., Vignaud, P., Zollikofer, C., Brunet, M., 2005. Morphological affinities of the *Sahelanthropus tchadensis* (Late Miocene hominid from Chad) cranium. *Proc. Natl. Acad. Sci.* 102, 18836–18841.
- Holm, S., 1979. A simple sequentially rejective multiple test procedure. *Scand. J. Stat.* 6, 65–70.
- Kimbel, W.H., Rak, Y., 2010. The cranial base of *Australopithecus afarensis*: new insights from the female skull. *Philos. Trans. R. Soc. B* 365, 3365–3376.
- Kimbel, W.H., White, T.D., 1988. Variation, sexual dimorphism and the taxonomy of *Australopithecus*. In: Grine, F.E. (Ed.), *Evolutionary History of The “Robust” Australopithecines*. Aldine de Gruyter, New York, pp. 175–192.
- Kimbel, W.H., Rak, Y., Johanson, D.C., 2004. *The Skull of Australopithecus afarensis*. Oxford University Press, New York.
- Kimbel, W.H., Suwa, G., Asfaw, B., Rak, Y., White, T.D., 2014. *Ardipithecus ramidus* and the evolution of the human cranial base. *Proc. Natl. Acad. Sci.* 111, 948–953.
- Klingenberg, C.P., 2011. MORPHOJ: an integrated software package for geometric morphometrics. *Mol. Ecol. Resour.* 11, 353–357.
- Le Gros Clark, W.E., 1955. Reason and fallacy in the study of fossil man. *Discovery* 16, 7–15.
- Ledogar, J.A., Dechow, P.C., Wang, Q., Gharpure, P.H., Gordon, A.D., Baab, K.L., Smith, A.L., Weber, G.W., Grosse, I.R., Ross, C.F., Richmond, B.G., Wright, B.W., Byron, C., Wroe, S., Strait, D.S., 2016. Human feeding biomechanics: performance, variation, and functional constraints. *PeerJ* 4, e2242.
- Ledogar, J.A., Benazzi, S., Smith, A.L., Weber, G.W., Carlson, K.B., Dechow, P.C., Grosse, I.R., Ross, C.F., Richmond, B.G., Wright, B.W., Wang, Q., Byron, C., Carlson, K.J., De Ruiter, D.J., Pryor McIntosh, L.C., Strait, D.S., 2017. The biomechanics of bony facial “buttresses” in South African australopiths: an experimental study using finite element analysis. *Anat. Rec.* 300, 171–195.
- Leslie, E.R., Shea, B.T., 2016. Gibbons to gorillas: Allometric issues in hominoid cranial evolution. In: Reichard, U.H., Hirai, H., Barelli, C. (Eds.), *Evolution of Gibbons and Siamang*. Developments in Primatology: Progress and Prospects. Springer, New York, pp. 185–203.
- Lieberman, D.E., Carlo, J., Ponce de León, M., Zollikofer, C.P.E., 2007. A geometric morphometric analysis of heterochrony in the cranium of chimpanzees and bonobos. *J. Hum. Evol.* 52, 647–662.
- McCollum, M.A., 2000. Subnasal morphological variation in fossil hominids: a reassessment based on new observations and recent developmental findings. *Am. J. Phys. Anthropol.* 112, 275–283.
- McCollum, M.A., Grine, F.E., Ward, S.C., Kimbel, W.H., 1993. Subnasal morphological variation in extant hominoids and fossil hominids. *J. Hum. Evol.* 24, 87–111.
- Neaux, D., 2017. Morphological integration of the cranium in *Homo*, *Pan*, and *Hylobates* and the evolution of hominoid facial structures. *Am. J. Phys. Anthropol.* 162, 732–746.
- Neaux, D., Guy, F., Gilissen, E., Coudyzer, W., Ducrocq, S., 2013. Covariation between midline cranial base, lateral basicranium, and face in modern humans and chimpanzees: a 3D geometric morphometric analysis. *Anat. Rec.* 296, 568–579.
- Nevell, L., Wood, B., 2008. Cranial base evolution within the hominin clade. *J. Anat.* 212, 455–468.
- R Development Core Team, 2016. *R: A language and environment for statistical computing*. R Foundation for Statistical Computing, Vienna, Austria.
- Rak, Y., 1983. *The Australopithecine Face*. Academic Press, New York.
- Rak, Y., Marom, A., 2017. Opposing extremes of zygomatic bone morphology: *Australopithecus boisei* versus *Homo neanderthalensis*. *Anat. Rec.* 300, 152–159.
- Remis, M.J., 1998. The gorilla paradox. In: Strasser, E., Feagle, J.G., Rosenberger, A.L., McHenry, H.M. (Eds.), *Primate Locomotion*. Springer, New York, pp. 95–106.
- Rohlf, J.F., 2015. The tps series of software. *Hystrix* 26, 9–12.
- Ross, C., Henneberg, M., 1995. Basicranial flexion, relative brain size, and facial kyphosis in *Homo sapiens* and some fossil hominids. *Am. J. Phys. Anthropol.* 98, 575–593.
- Russo, G.A., Kirk, E.C., 2013. Foramen magnum position in bipedal mammals. *J. Hum. Evol.* 65, 656–670.
- Russo, G.A., Kirk, E.C., 2017. Another look at the foramen magnum in bipedal mammals. *J. Hum. Evol.* 105, 24–40.
- Ruth, A.A., Raghanti, M.A., Meindl, R.S., Lovejoy, C.O., 2016. Locomotor pattern fails to predict foramen magnum angle in rodents, strepsirrhine primates, and marsupials. *J. Hum. Evol.* 94, 45–52.
- Sansalone, G., Kotsakis, T., Piras, P., 2016. New systematic insights about Plio-Pleistocene moles from Poland. *Acta Palaeontol. Pol.* 61, 221–229.
- Schaefer, M.S., 1999. Brief communication: foramen magnum-carotid foramina relationship: is it useful for species designation? *Am. J. Phys. Anthropol.* 110, 467–471.
- Schneider, C.A., Rasband, W.S., Eliceiri, K.W., et al., 2012. NIH Image to ImageJ: 25 years of image analysis. *Nat. Methods* 9, 671–675.
- Schultz, A.H., 1942. Conditions for balancing the head in primates. *Am. J. Phys. Anthropol.* 29, 483–497.
- Schwartz, J.H., Tattersall, I., 2005. *The Human Fossil Record. Volume 4. Craniodental Morphology of Early Hominids (Genera Australopithecus, Paranthropus, Orrorin), and Overview*. Wiley-Liss, New York.
- Shea, B.T., 1983. Allometry and heterochrony in the African apes. *Am. J. Phys. Anthropol.* 62, 275–289.
- Smith, A.L., Benazzi, S., Ledogar, J.A., Tamvada, K., Pryor Smith, L.C., Weber, G.W., Spencer, M.A., Lucas, P.W., Michael, S., Shekeban, A., Al-Fadhalah, K., Almusallam, A.S., Dechow, P.C., Grosse, I.R., Ross, C.F., Madden, R.H., Richmond, B.G., Wright, B.W., Wang, Q., Byron, C., Slice, D.E., Wood, S., Dzialo, C., Berthaume, M.A., van Casteren, A., Strait, D.S., 2015. The feeding biomechanics and dietary ecology of *Paranthropus boisei*. *Anat. Rec.* 298, 145–167.
- Suwa, G., Asfaw, B., Kono, R.T., Kubo, D., Lovejoy, C.O., White, T.D., 2009. The *Ardipithecus ramidus* skull and its implications for hominid origins. *Science* 326, 68e1–68e7.
- Thorpe, S.K.S., Crompton, R.H., 2006. Orangutan positional behavior and the nature of arboreal locomotion in Hominoidea. *Am. J. Phys. Anthropol.* 131, 384–401.
- Tobias, P.V., 1967. *Olduvai Gorge, Vol. 2, The Cranium and Maxillary Dentition of Australopithecus (Zinjanthropus) boisei*. Cambridge University Press, London.
- Topinard, P., 1878. *Anthropology*. J.B. Lippincott and Co., Philadelphia.
- Weber, G.W., Krenn, V.A., 2017. Zygomatic root position in recent and fossil hominids. *Anat. Rec.* 300, 160–170.
- White, T.D., Suwa, G., Asfaw, B., 1994. *Australopithecus ramidus*, a new species of early hominid from Aramis, Ethiopia. *Nature* 371, 306–312.
- Wroe, S., Ferrara, T.L., McHenry, C.R., Curnoe, D., Chamoli, U., 2010. The cranio-mandibular mechanics of being human. *Proc. Roy. Soc. Lond. B* 277, 3579–3586.
- Zollikofer, C.P.E., Ponce de León, M.S., Lieberman, D.E., Guy, F., Pilbeam, D., Likius, A., Mackaye, H.T., Vignaud, P., Brunet, M., 2005. Virtual cranial reconstruction of *Sahelanthropus tchadensis*. *Nature* 434, 755–759.